

Electronic structure of single DNA molecules resolved by transverse scanning tunnelling spectroscopy

ERREZ SHAPIR¹, HEZY COHEN¹, ARRIGO CALZOLARI², CARLO CAVAZZONI^{2,3}, DMITRY A. RYNDYK⁴, GIANAURELIO CUNIBERTI^{4*}, ALEXANDER KOTLYAR⁵, ROSA DI FELICE^{2†} AND DANNY PORATH^{1†}

¹Physical Chemistry Department and Center for Nanoscience and Nanotechnology, The Hebrew University, Jerusalem 91904, Israel

²National Center on nanoStructures and bioSystems at Surfaces (S3) of INFN-CNR, Via Campi 213/A, 41100 Modena, Italy

³CINECA, Via Magnanelli 6/3, 40033 Casalecchio di Reno Bologna, Italy

⁴Institute for Theoretical Physics, University of Regensburg, D-93040 Regensburg, Germany

⁵Department of Biochemistry George S. Wise Faculty of Life Sciences and Nanotechnology Center Tel Aviv University, Ramat Aviv 69978, Israel

*Present address: Institute for Materials Science and Max Bergmann Center for Biomaterials, Dresden University of Technology, D-01069 Dresden, Germany

†e-mail: rosa@unimore.it; porath@chem.ch.huji.ac.il

Published online: 25 November 2007; doi:10.1038/nmat2060

Attempts to resolve the energy-level structure of single DNA molecules by scanning tunnelling spectroscopy span over the past two decades, owing to the unique ability of this technique to probe the local density of states of objects deposited on a surface. Nevertheless, success was hindered by extreme technical difficulties in stable deposition and reproducibility. Here, by using scanning tunnelling spectroscopy at cryogenic temperature, we disclose the energy spectrum of poly(G)–poly(C) DNA molecules deposited on gold. The tunnelling current–voltage (I – V) characteristics and their derivative (dI/dV – V) curves at 78 K exhibit a clear gap and a peak structure around the gap. Limited fluctuations in the I – V curves are observed and statistically characterized. By means of *ab initio* density functional theory calculations, the character of the observed peaks is generally assigned to groups of orbitals originating from the different molecular components, namely the nucleobases, the backbone and the counterions.

The electrical properties of single double-stranded DNA molecules have attracted great interest in the past two decades, leading to a series of experiments^{1–3} to study the electron transfer and conduction through single DNA molecules and in various aggregation forms^{4,5}. Nearly all of the single-molecule experiments addressed the conductivity along molecules that are attached to electrodes at the molecule ends. Besides fixing many chemical and physical properties, the intrinsic electronic structure of an object also determines its response to an external electric field. Hence, it is desirable to get this knowledge for DNA to understand its suitability to support electrical currents and the viable transport mechanisms. Scanning tunnelling spectroscopy (STS) is the technique of choice for measuring the electronic density of states (DOS) of a single molecule⁶, as was demonstrated through the years for various carbon nanostructures^{7,8}, molecular objects⁹ and inorganic nanoparticles¹⁰ deposited on substrates.

Following the invention of the scanning tunnelling microscope (STM) in 1982, there was a substantial number of attempts to measure single DNA molecules using STM. However, whereas several groups showed high-resolution images with quite detailed structure of the DNA molecules^{11–18}, direct tunnelling spectroscopy across the helices was reported only a few times^{18–21} and clear interpretation was inhibited by technical hurdles²². In all of these studies, DNA–salt aggregates or very short DNA oligomers with no clear orientation were measured. Moreover, the STS measurements of DNA were always done at room temperature, making it impossible to resolve the electronic levels within the thermal noise.

Theoretical predictions for the DNA electronic structure, commonly based on molecular quantum mechanics calculations such as density functional theory^{23,24} (DFT) or Hartree–Fock²⁵, cannot be conclusive. In fact, the lack of clear experimental data for single DNA molecules hinders the establishment of the theories. Experimental data such as optical spectra, in which a structure of one broad peak of the coupled levels is observed^{26,27}, are not refined enough to determine the single-molecule electronic structure.

Here, we present STS results on long homogeneous single novel poly(G)–poly(C) DNA molecules²⁸ deposited on gold¹³: such results enable us for the first time to resolve conductance peaks that are associated with the electronic levels of the nucleic acids. In parallel, insight into the nature of such levels is gained by *ab initio* DFT calculations for the very same base sequence, eventually enabled by the existence of clear experimental data. We thus establish a combined method to unravel the electronic structure of single DNA molecules.

STS⁶ is an electrical measurement through a tunnel junction, in which the current I between the STM tip and the sample is characterized as a function of the voltage V (providing I – V characteristics). The tunnel current I between the tip and the surface may be expressed⁶ as:

$$I = A \int_{-\infty}^{\infty} D_s(r, E) D_t(E - eV) |T(E, V, r)|^2 \times [f(E - eV) - f(E)] dE, \quad (1)$$

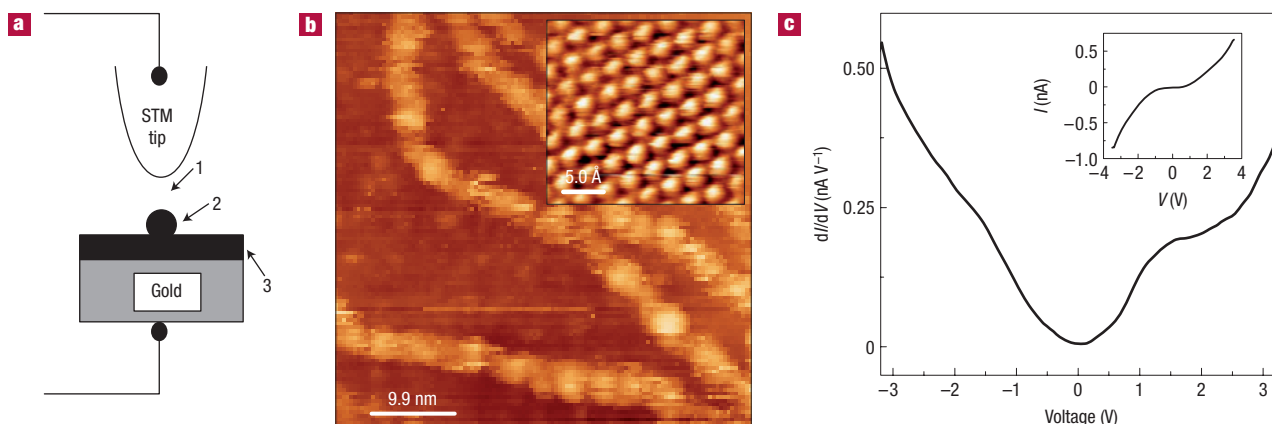


Figure 1 The measurement scheme, DNA STM image and STS on bare gold. **a**, Schematic diagram of the double-barrier tunnel junction configuration. The first tunnel junction is formed between the STM tip and the molecule (indicated as 1). The DNA molecule profile is marked as 2 and the second junction (marked as 3) is between the molecule and the gold surface. **b**, Room-temperature STM image of poly(G)–poly(C) DNA molecules on which STS measurements were carried out. The full length of the DNA molecules shown here is about 1.2 μm . The inset shows an atomic-resolution image of a bare gold part of the surface (scanned at $T \sim 78$ K), verifying the cleanliness of the STM tip and surface. **c**, A typical (dI/dV) – V curve measured on bare gold (corresponding I – V curve in the inset), showing the gapless characteristic of the substrate.

where the subscripts s and t indicate the surface and tip, respectively. E is the energy relative to the Fermi level and V is the applied voltage, f is the Fermi function, $|T|^2$ is the tunnelling probability, A is a proportion coefficient and D is the DOS (depending on both the energy E and the position r). At $T = 0$ K, expression (1) becomes simpler:

$$I = A \int_0^{eV} D_s(r, E) D_t(E - eV) |T(E, V, r)|^2 dE, \quad (2)$$

where $|T|^2$ can be written in terms of the sample and tip workfunctions and of the tip–sample separation. If the bias-voltage dependence of $|T|^2$ is weak, the derivative of expression (2) is $dI/dV \propto D_s(r, eV) D_t(0)$. The latter relation provides straightforward information on the electron local DOS of the sample under the tip position. In principle, the full complexity of the double-junction geometry should be taken into account in the theoretical evaluation for a more rigorous handling of the scattering term $|T(e, V, r)|^2$ in the integral (2), so that not only the DOS of the measured object determines the tunnelling current and quantum conductance, but also the contacts and the whole configuration. Thus, in the most general case, non-equilibrium effects due to the voltage dependence in the integral (2), as well as Coulomb blockade contributions, could be responsible for deviations of the conductance curves with respect to the ground-state molecular DOS (for example, shifts of the peaks and adjustment of their intensities). However, as a first level of interpretation, we provide here an explanation of the conductance curves on the basis of the DOS, which is the only approach feasible from first principles. More complex treatments of the measurement geometry require recourse to semi-empirical methods. We note that, as we discuss below, we at least verified that Coulomb blockade effects are not a major factor in the adopted measurement conditions for this study.

The measurement configuration on the double-stranded DNA is a double-barrier tunnel junction (Fig. 1a), meaning that when the STM tip is mounted above the molecule while measuring, two tunnel junctions are formed: one between the tip and the molecule and the other between the molecule and the surface. The latter can be formed, for example, by the insulating

backbone of the molecules themselves. Figure 1b shows an image of poly(G)–poly(C) DNA molecules acquired before STS measurements. The image shows segments of poly(G)–poly(C) DNA molecules (which are up to about 1.2 μm long), where a periodic structure is clearly seen¹³. The surrounding surface, magnified in the inset at atomic resolution, appears clean and features of the gold (111) surface are visible (for example, atomic terraces). This is important for ensuring reliable STS measurements and avoiding artefacts due to contamination. Figure 1c shows a typical (dI/dV) – V curve on the bare gold (at the same conditions), showing a smooth gapless structure, and the corresponding I – V measurement is shown in the inset.

Only DNA molecules that appeared intact in the topographic images were selected for STS measurements, which were always carried out on the top of one of the molecule ‘bulbs’ (Fig. 1b). Figure 2a–d shows four groups of I – V curves measured on four different double-stranded DNA molecules. The corresponding conductance curves (dI/dV) – V of the average I – V curve of each group (Fig. 2e–h) clearly show the existence of an excitation gap and emphasize the details of the peak structures. The average gap width for the four cases is 2.5 eV at $T \sim 78$ K. The peaks in the conductivity curves (Fig. 2e–h) are numbered from 1 to 3 in each of the positive and negative bias ranges. The six peaks in each conductivity curve contain information about the electronic structure of double-stranded DNA molecules when deposited on the surface. They appear quite broad, probably owing to structural disorder and thermal broadening, and may be divided into more peaks that are indistinguishable within the experimental resolution at this temperature. Table 1 summarizes the values of the gap widths and peak energies. The experimental I – V characteristics are fairly reproducible at $T \sim 78$ K. The gap also shows reproducibility at 300 K and the average gap value does not change within the temperature range 300–78 K.

To establish that the above experimental data of our STS measurements indeed represent the specific DOS of the DNA molecules that we measured, and to identify the variability of the peaks and of the gap within the collected data, a statistical analysis was carried out on the I – V gap-width and peak-energy values. For the statistics, we included a larger data set of ~ 180 I – V curves (using their corresponding conductivity curves). Each one

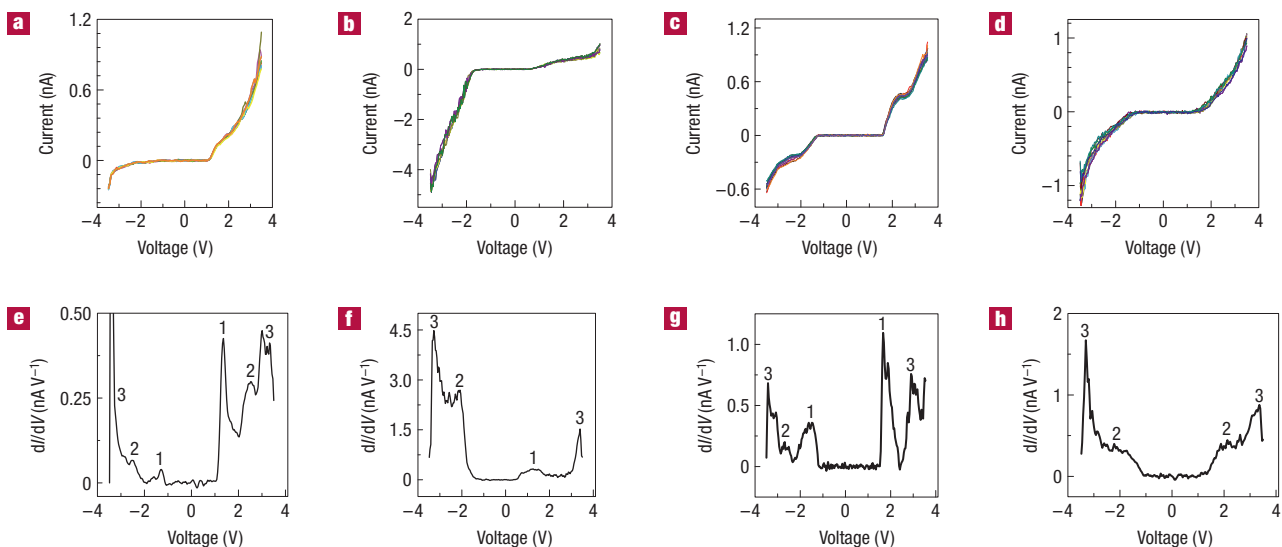


Figure 2 Current–voltage and conductance curves from the STS measurements. STS measurements presented as I – V and corresponding derivative (dI/dV)– V characteristics. **a–d**, I – V sets (containing 10, 12, 16 and 14 curves respectively) taken at $T \sim 78$ K. Each of the I – V sets corresponds to a different poly(G)–poly(C) DNA molecule. **e–h**, The corresponding derivatives of the average I – V of each set. The average gap is ~ 2.5 eV (see Table 1). The measurements were done with V_{bias} of 2.8 V and I_{set} of 0.5 nA.

Table 1 Summary of the STS results for poly(G)–poly(C) DNA taken at $T \sim 78$ K. The measurement uncertainty due to white noise was ± 0.2 V. The ‘statistics data’ column shows values of the weighted averages of the peak position at the energy axes and gap-width distributions found in the statistical analysis of 180 different measurement sets.

	Peak no.	Curve (a)	Curve (b)	Curve (c)	Curve (d)	Average of the 4 cases	Statistics data	Deviation (V)
Negative-voltage peak positions (V)	1	–1.3	–	–1.6	–	–1.5	–1.4	± 0.2
	2	–2.5	–2.3	–2.5	–2.3	–2.4	–2.5	± 0.2
	3	–3.4	–3.3	–3.5	–3.3	–3.4	–3.3	± 0.2
Positive-voltage peak positions (V)	1	1.3	1.3	1.6	–	1.4	1.4	± 0.2
	2	2.5	–	–	2.2	2.4	2.4	± 0.2
	3	3.3	3.3	3.3	3.4	3.3	3.2	± 0.2
Voltage gap (V)		2.5	2.8	2.3	2.4	2.5	2.5	± 0.2

of these curves is an average of at least 10 very reproducible individual consecutive curves, as shown in Fig. 2, taken on different molecules. Figure 3 shows the statistics results: the histograms of the peak-energy and gap-width distributions are shown in Fig. 3a and b, respectively. The peak-energy distribution shows six distinguishable groups (Fig. 3a): three in the negative and three in the positive bias range (numbered from 1 to 3 in each bias range). Each group in this peak distribution differs energetically from its neighbouring groups by at least 0.2 eV, which is beyond the uncertainty limit in our results due to noise. The weighted averages of the groups in the peak-energy distribution (Fig. 3a) and gap-width distribution (Fig. 3b) show a good correlation with the results shown in Fig. 2 (details in Table 1), namely there is a good approximation between the statistics and the individual results. In particular, the peak positions for four molecules do not deviate much from the average peak positions of the large data set, indicating that variations from molecule to molecule and variations in the attachment of the DNA to the surface at different positions do not alter the spectra beyond a limited variability. Preliminary STS results obtained by doping the poly(G)–poly(C) in a ratio of one Ag^{2+} ion per base pair show that the average gap widths are reduced by $\sim 25\%$. This change in the STS spectra by altering the

composition and structure of the DNA is further proof that our measurements probe the deposited molecules and are sensitive to their electronic structure.

To support our assumption that the measured conductance curves approximately reflect the sample DOS according to expression (2), although the measurement is collected at finite temperature, it is desirable to assign the peaks to molecular electron states^{7,8}. Simulations of I – V and (dI/dV) – V curves were so far done by empirical models, namely by using tight-binding hamiltonians with parameters either fixed through experimental fitting²⁹ or taken from *ab initio* calculations. In the former case, the charge distribution of each electronic state remains elusive, because only the energy levels and the gaps are fitted. In the latter case, the nature of the electron states is known from the *ab initio* calculations: however, only those states that are included in the model will play a role. For instance, if we assume that only the bases³⁰ contribute to the electron tunnelling with no role of the backbone and counterions, this assumption will affect the results.

To circumvent these restrictions, we carried out a fully *ab initio* simulation of a poly(G)–poly(C) periodic wire, as similar as possible to the experimental samples, although with necessary approximations. We neglected the solvent but included

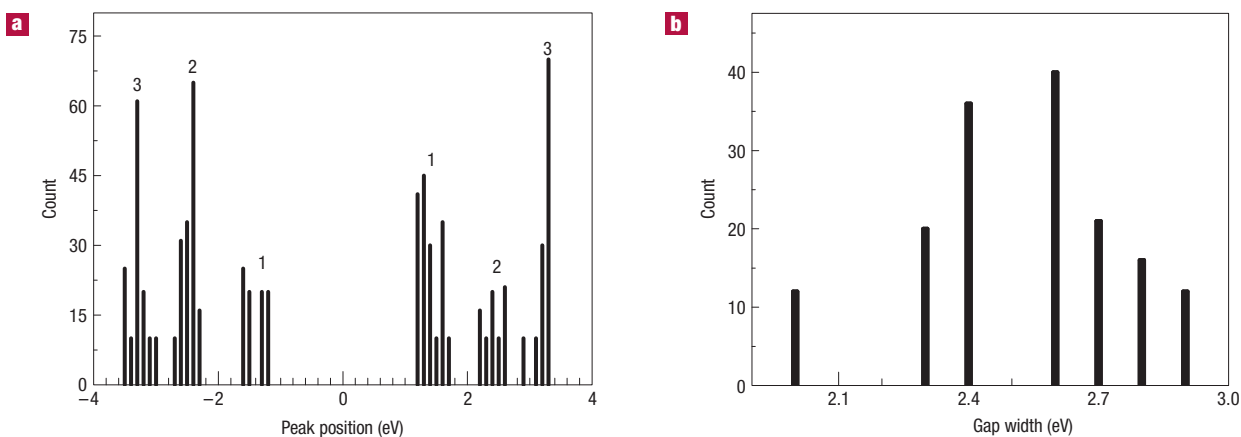


Figure 3 Statistical analysis of the experimental STS results. **a,b**, Statistical analysis of the peak-energy values (**a**) and of the fundamental energy gap (**b**), taken from 180 experimental curves (each curve in the statistics is an average of at least 10 consecutive individual similar I - V curves taken at different molecules).

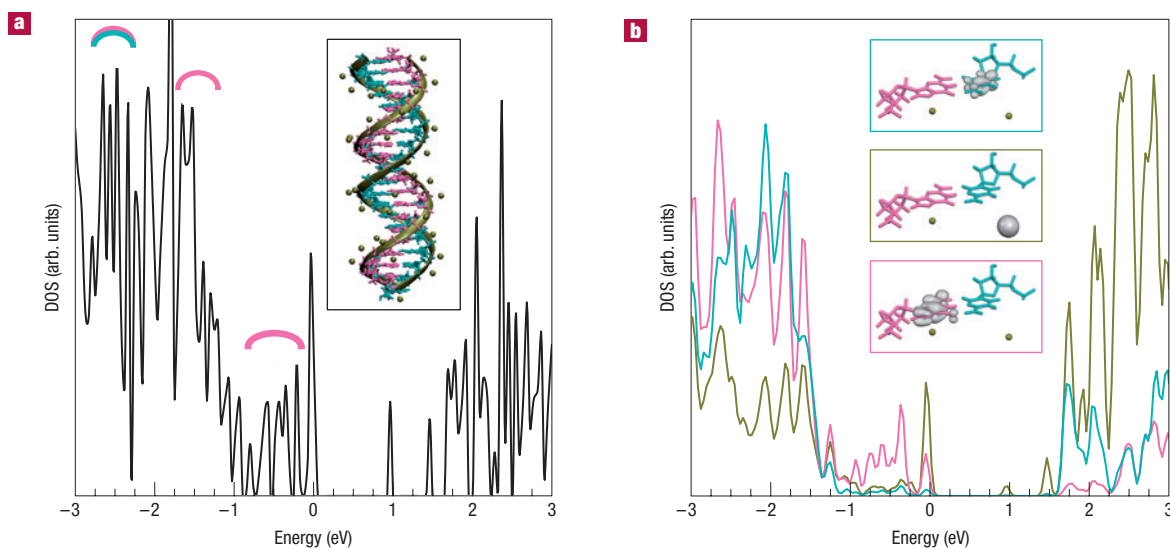


Figure 4 Simulated structures and computed DOS. The energy origin along the horizontal axes of both DOS plots is set at the level of the highest occupied eigenvalue. **a**, Plot of the electronic total DOS. From a thorough analysis of the character of electron states, similar states can be grouped into gross convoluted features at -0.5 eV, -1.5 eV and -2.5 eV. (Arches are shown as a guide to the eye; the origin of the energy scale is set at the top of the occupied levels, so the absolute values of the peak energies are shifted with respect to the experimental peaks.) The inset shows a three-dimensional representation of the simulated structure. The periodic unit cell contains 10 GC pairs and 2 replicas are shown here. Pink and cyan frames represent guanine and cytosine bases, respectively. The backbone is shown as ribbons and the external green spheres are the Na^+ counterions included in the simulation. **b**, Atom-projected DOS on guanine, cytosine and Na, with the same colour scheme as used for the atomic structures. The highest occupied peak originates from the guanine HOMO, as demonstrated by the G character (pink) of the peak: a projection of the state on a single GC pair is shown in the lowest inset. The first unoccupied levels (green peak at ~ 0 eV) are due to the Na^+ counterions (middle inset), and spuriously appear at an energy coincident with that of the G HOMO, owing to DFT and to the lack of screening solvent²⁴. They should be shifted to the middle of the gap, by a quantity whose determination is beyond present computational limits. The first C unoccupied states (top inset) are separated from the highest occupied levels by a DFT gap of ~ 2.5 eV (measured between the centres of the G and C broad peaks).

the backbone and Na^+ counterions in the simulation (Fig. 4a). We are aware that the solvent may also play a role in pinning the electron levels, but this issue is still controversial and is addressed elsewhere^{31,32}, and it is not expected to compromise the essence of our results (see the discussion on the water effects in the Supplementary Information). Previous similar simulations were done for the same poly(G)-poly(C) sequence without including the counterions²³: it was found that the fundamental

bandgap is only due to the guanine (G) and cytosine (C) bases. By including the counterions in a simulation for a polymer with a different poly(GC)-poly(CG) sequence²⁴, it was instead found that the counterions contribute novel empty electron states in the fundamental gap between the G and C states. The question is then: do such counterion-induced electronic levels contribute to the peaks in the (dI/dV) - V curves measured by STS?

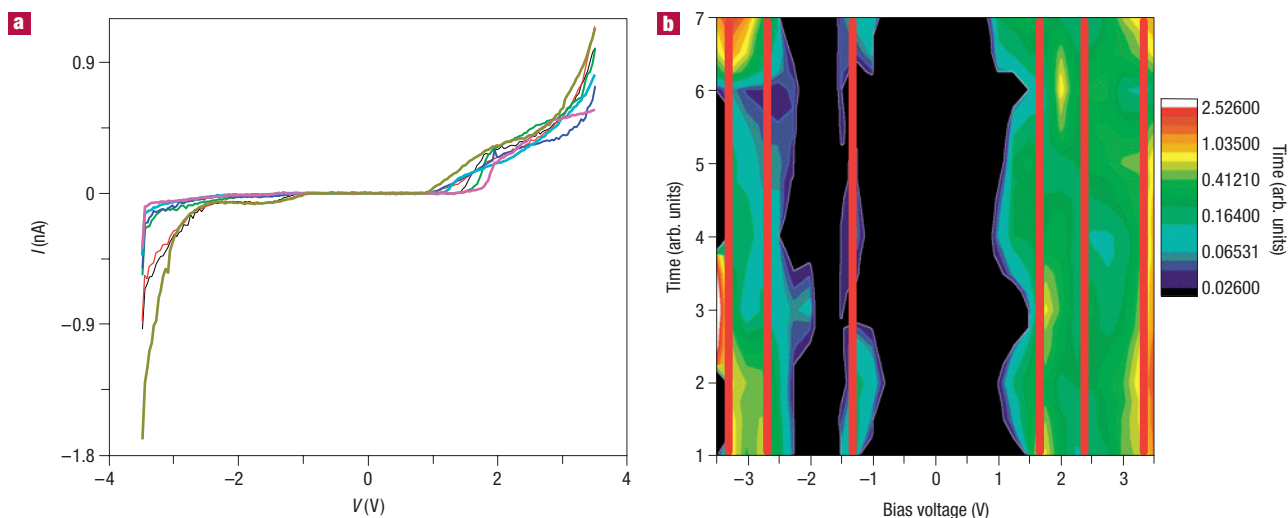


Figure 5 Reproducibility of the experimental STS curves over ‘time’. **a**, Seven average I - V curves obtained by grouping into seven sets the several consecutive curves collected for this analysis: each average contains 9 to 25 curves. **b**, ‘Time’ evolution of the spectroscopic signal. The logarithmic colour map represents the conductance as a function of voltage (horizontal axis) and of ‘time’ (vertical axis). The grid on the ‘time’ axis is defined only at integer values. The vertical lines are drawn as a guide to the eye to locate the conductance peaks: the peak energies practically coincide with the values in Table 1. The conductance corresponds to the seven subsequent I - V curves in **a**.

The computed total and atom-projected density of states are plotted in Fig. 4. The figure demonstrates that the counterions (green curve) indeed contribute new empty electron states in the gap between the G (~ -0.5 eV) and the C (~ 2 eV) peaks, with a very low DOS relative to the G and C features, yet a finite number of discrete levels scattered throughout the G–C gap and roughly centred around 1 eV. Let us now discuss why the Na^+ levels, which are a direct output of our calculations, may help explain the observations, contrary to unsatisfactory attempts that are based only on the ground-state electronic structure on G and C. *Ab initio* DFT electronic structure calculations of G-rich DNA polymers usually report a π - π^* G–C energy gap of ~ 2 – 3 eV, depending on the exact polymer sequence and computational details^{23,24,30,31}, consistent with our findings. Taking into account that ground-state DFT results underestimate the gap between occupied and unoccupied states by as much as 100% and even more, the measurement of an average fundamental gap of ~ 2.5 eV (Table 1) cannot be explained naively in terms of a G–C gap, because the theoretical prediction should be shifted to roughly 5–6 eV. Hence, alternative explanations must be called for. If the ground-state DOS of an isolated DNA polymer is representative of the measured STS curves, then our and other²⁴ results indicate that the first unoccupied levels are due to the counterions that contribute ‘localized’ states (as opposite to ‘extended’) in the G–C gap, as indicated by the present computational outcome. Although the low density of the Na^+ states raises the question of whether they are detectable in STS measurements, such states explain a shrink of the computed gap, which can match with the experimental determination if the proper correction to the DFT value is applied. For the occupied portion of the theoretical spectra, the energy differences between the main DOS features (convolutions centred roughly at -0.5 eV, -1.5 eV and -2.5 eV in Fig. 4a) are roughly consistent with energy differences between the three peaks at negative energies in the experimental spectra. They are due mainly to guanine orbitals, with cytosine orbitals starting to contribute at the lowest energies. Each gross feature in the computed DOS is a collection of several discrete levels localized at multiple helix planes: this should be the origin of the fine structure (not precisely

resolved) of the experimental peaks. We note that this is just a general comparison of the calculation with the STS peaks and not a one-to-one assignment.

We point out some effects that may be included in the theory to attain a rigorous comparison with the measured data, not currently feasible from first principles. As STS probes the molecular DOS when a hole is added in the occupied states or an electron in the empty states, excited-state and non-equilibrium effects may be non-negligible. In such a case, quasiparticle corrections and tunnelling currents under applied bias should be evaluated and ground-state DFT results on the DOS cannot be plainly applied to interpret the spectroscopic peaks. Furthermore, structural deformations due to the fact that the molecules lie flat on the surface and are surrounded by a solvation shell may be important: it may be that in the resulting polymer conformations the G–C gap is greatly lowered with respect to the isolated-molecule phase, and the STS indeed probes only G and C levels. This cannot be concluded, however, solely on the basis of ground-state DFT calculations for isolated polymers that contain only the bases. These issues are premature at the present stage of experimental and theoretical development (see the Supplementary Information). In any case, our results demonstrate that for a reliable theory all of the components of the polymer are important.

In most cases, the experimental results were highly reproducible, as demonstrated by the statistics. In some cases, however, when measuring tens of consecutive curves at the same position, we observed some kind of ‘switching’ back and forth between repeating I - V characteristics. Seven consecutive groups (9–25 curves in each group) of nearly identical I - V curves were averaged and plotted in seven sets assigned to consecutive ‘time’ instants. Figure 5a shows how the current plot in a certain curve switches from one I - V shape to another and back to partial overlap with the previous shape. Figure 5b further shows the phenomenon and the ‘time’ repetition by plotting a logarithmic colour map of the conductivity, related to the curves in Fig. 5a, as a function of the bias voltage and the ‘time’. The conductivity values are identified by different colours according to the scale in the legend. The peaks in the dI/dV - V curves can therefore

be identified with the red/orange, yellow and green spots in this colour map (see Fig. 5b). Note the peaks that appear, disappear and reappear along the vertical direction ('time'). To emphasize the repetitions along the timescale, vertical lines are drawn, along which the repetitions occur.

The contribution of single-electron tunnelling effects^{8,33} to the fluctuation in the I - V gaps and peaks is believed to be small in comparison with the observed voltage gaps. When the capacitance of the tip-molecule junction is much smaller than that of the molecule-substrate junction, as it is believed to be in this case (checked by current-distance measurements), the latter junction is the fast one and the incoming charge rapidly tunnels out and charging effects are not observed¹⁰. Moreover, small changes in I_{set} during STS measurements on particles would change their residual charge, Q_0 , and cause a variation in the Coulomb blockade voltage gap^{8,33}. Typically, in our measurements, these variations are negligible with respect to the range of the observed gap widths (2.0–2.9 eV), ruling them out as a possible source of the observed conductance fluctuations, and leaving structural fluctuations or changes of the molecule-substrate contact as the most likely origin. For comparison, previous STS data on semiconductor nanorods (CdSe with diameters of 3.5–7 nm)³⁴ showed that the contribution of single-electron tunnelling effects (~ 0.16 eV) was less than 10% of the nanorod energy gap (~ 2.4 eV measured as the voltage gap). We note that the ratio of capacitances in the asymmetric junction, as mentioned above, also rules out the possibility that some similarity in the peak positions on both sides of the gap originates from the same set of highest occupied molecular orbital (HOMO) or lowest unoccupied molecular orbital levels and we assume that measurements at a lower temperature may remove this similarity and resolve the substructure of the peaks.

Here, we determined the main groups of energy levels and the energy gap in the electronic structure of novel poly(G)-poly(C) DNA molecules adsorbed on a metal surface using STS. We found that the energy gap in the I - V curves does not show significant temperature dependence. The peaks in the dI/dV - V curves were identified as fingerprints of the discrete energy spectrum in the molecules. With the help of *ab initio* calculations, the peaks at negative voltage were generally ascribed to the HOMOs of the nucleobases. In addition, we showed that to explain the measured positive-voltage peaks, we need to go beyond the simplest ground-state DFT framework that accounts only for the free nucleobases: a possible explanation within a ground-state approach is the role of counterions.

METHODS

SAMPLE PREPARATION, TIPS AND MEASUREMENT DETAILS

Each sample was prepared with a 10 μl drop of 10 nM poly(G)-poly(C) DNA (in Tris-acetate buffer, pH = 7), diluted in 18 M Ω distilled water (ratio of 1:20) and then deposited on a flame-annealed gold (111) surface. In part of the depositions, a voltage of 180 mV was applied to the metal substrate for ~ 15 min to attract the DNA to the surface electrostatically. Immediately after deposition, the sample was either imaged with an atomic force microscope to check the DNA topography and concentration on the surface (~ 1 – 10 molecules in $1 \times 1 \mu\text{m}^2$) and then the sample was inserted into the STM ultrahigh vacuum (UHV) chamber or directly after preparation inserted into the UHV chamber. The chamber pressure in our system was kept at $\sim 5 \times 10^{-11}$ mbar: note that in this UHV condition, the molecules are still thought to maintain a thin solvation shell, whose conformation is, however, unknown and probably quite different from the solution environment. The tips used in the study are standard Omicron chemically etched tungsten tips. The tips were kept in a desiccator, inserted into the vacuum chamber before use and mounted. At the beginning of each measurement session and when necessary, the tips were cleaned by a high-voltage pulse. The tips were then tested by the image quality and by STS on clean gold. We note that when a contaminant (for example, organic material) is attached to the tip apex or when a double tip is formed, it is

easily observable in the imaging and the spectroscopy and the above procedure is then used. STS measurements of current-voltage (I - V) curves were carried out during constant-current STM imaging to monitor that the electrical measurements pertain to single DNA molecules. The spectroscopy results were compared for different tips and the results were found to be similar. The reported images were taken with a current setpoint of 20–50 pA and a bias voltage of 2.5–2.8 V. The spectroscopy was carried out after setting the current setpoint to 0.5 nA and the bias voltage to 2.8 V, before disconnecting the feedback. The specific measured part of the DNA molecule was topographically scanned before and after the I - V measurement to verify that it remained intact and that the STM tip position was unchanged. We note that it is difficult to always obtain good samples and our procedure does not always yield samples with a high enough density of molecules. We also obtained samples in which the imaging was convincing but the I - V curves were noisy or the molecules were swept away by the tip. In our statistics, we included only sets of measurements where the molecules appeared identical and unperturbed by the tip before and after imaging and in which we measured a set of at least 10 consecutive reproducible curves and excluded sets that included noisy curves. The rest of the data are, however, generally consistent with the reported data.

DFT COMPUTATIONAL DETAILS

The calculations were done in the framework of DFT with the CP/FPMD (Car-Parrinello/first-principle molecular dynamics) package^{35,36} of the Quantum-ESPRESSO suite of codes, at <http://www.quantum-espresso.org>. We used the PBE³⁷ (Perdew-Burke-Ernzerhof) exchange-correlation functional, ultrasoft pseudopotentials³⁸ to represent the ion cores (only the valence electrons were treated explicitly: $1s^1$, $2s^2 2p^2$, $2s^2 2p^3$, $2s^2 2p^4$, $3s^1$, $3s^2 3p^3$ for H, C, N, O, Na, P; nonlinear core corrections were added for Na), and a plane-wave basis set with a kinetic energy cutoff of 25 Ryd for the wavefunctions and 200 Ryd for the charge density. An infinite poly(G)-poly(C) polymer was simulated, by applying periodic boundary conditions to a unit supercell. The unit block contained 10 GC pairs and was constructed from a single GC pair using the package 3DNA (ref. 39). Na^+ counterions were added in the most negative locations around the backbone, to maximize the electrostatic attraction. Periodic replicas were laterally separated by a thickness of vacuum of ~ 12 Å. Before computing the electronic structure, the atomic configuration was relaxed with a quenched Car-Parrinello dynamics until the forces were smaller than 0.06 eV \AA^{-1} . The simulation box contained 650 atoms: such a large size puts this plane-wave calculation at the forefront of the current feasibility on parallel supercomputers, if we want to use a completely unbiased basis set as the plane waves, and fully *ab initio* ingredients.

Received 30 April 2007; accepted 15 October 2007; published 25 November 2007.

References

- Ratner, M. A. Photochemistry: Electronic motion in DNA. *Nature* **397**, 480–481 (1999).
- Taubes, G. Biophysics: Double helix does chemistry at a distance—But how? *Science* **275**, 1420–1421 (1997).
- Porath, D., Bezryadin, A., de Vries, S. & Dekker, C. Direct measurement of electrical transport through DNA molecules. *Nature* **403**, 635–638 (2000).
- Porath, D., Cuniberti, G. & Di Felice, R. Charge transport in DNA-based devices. *Topics Curr. Chem.* **237**, 183–227 (2004).
- Endres, R. G., Cox, D. L. & Singh, R. P. Colloquium: The quest for high-conductance DNA. *Rev. Mod. Phys.* **76**, 195–214 (2004).
- Wiesendanger, R. *Scanning Probe Microscopy and Spectroscopy* (Cambridge Univ. Press, Cambridge, 1994).
- Porath, D. & Millo, O. Single electron tunneling and level spectroscopy of isolated C_{60} molecules. *J. Appl. Phys.* **81**, 2241–2244 (1997).
- Porath, D., Levi, Y., Tarabiah, M. & Millo, O. Tunneling spectroscopy of isolated C_{60} molecules in the presence of charging effects. *Phys. Rev. B* **56**, 9829–9833 (1997).
- Huo, J. G. & Wang, K. D. Study of single molecules and their assemblies by scanning tunneling microscopy. *Pure Appl. Chem.* **78**, 905–933 (2006).
- Banin, U. & Millo, O. Tunneling and optical spectroscopy of semiconductor nanocrystals. *Annu. Rev. Phys. Chem.* **54**, 465–492 (2003).
- Binnig, G. & Rohrer, H. in *Proc. 6th General Conf. of the European Physical Society, Trends in Physics* Vol. 1 (eds Janta, J. & Pantoflicek, J.) 38 (European Physical Society, Prague, 1984).
- Binnig, G. & Rohrer, H. Scanning tunneling microscopy—from birth to adolescence. *Rev. Mod. Phys.* **59**, 615–625 (1987).
- Shapir, E. *et al.* High-resolution STM imaging of novel poly(dG)-poly(dC) DNA. *J. Phys. Chem. B* **110**, 4430–4433 (2006).
- Lindsay, S. M., Thundat, T. & Nagahara, L. A. Adsorbate deformation as a contrast mechanism in STM images of bio-polymers in an aqueous environment: Images of the unstained, hydrated DNA double helix. *J. Microsc.* **152**, 213–220 (1988).
- Wilson, T. E. *et al.* Scanning tunneling microscopy at high gap resistances and on chemically modified silicon surfaces. *J. Vac. Sci. Technol. B* **9**, 1171–1176 (1991).
- Youngquist, M. G., Driscoll, R. J., Coley, T. R., Goddard, W. A. & Baldeschwieler, J. D. Scanning tunneling microscopy of DNA: Atom-resolved imaging, general observations and possible contrast mechanism. *J. Vac. Sci. Technol. B* **9**, 1304–1308 (1991).
- Tanaka, H. & Kawai, T. Visualization of detailed structures within DNA. *Surf. Sci.* **539**, L531–L536 (2003).

18. Iijima, M. *et al.* STM/STS study of electron density of states at the bases sites in the DNA alternating copolymers. *Chem. Lett.* **34**, 1084–1085 (2005).
19. Lindsay, S. M. *et al.* Studies of the electrical properties of large molecular adsorbates. *J. Vac. Sci. Technol. B* **9**, 1096–1101 (1991).
20. Xu, M. S. *et al.* Conformation and local environment dependent conductance of DNA molecules. *Small* **1**, 1–4 (2005).
21. Xu, M. S. *et al.* Conductance of single thiolated poly(GC)–poly(GC) DNA molecules. *Appl. Phys. Lett.* **87**, 083902 (2005).
22. Clemmer, C. & Beebe, T. P. Graphite: A mimic for DNA and other biomolecules in scanning tunneling microscope studies. *Science* **251**, 640–642 (1991).
23. de Pablo, P. J. *et al.* Absence of dc-conductivity in λ -DNA. *Phys. Rev. Lett.* **85**, 4992–4995 (2000).
24. Gervasio, F. L., Carloni, P. & Parrinello, M. Electronic structure of wet DNA. *Phys. Rev. Lett.* **89**, 108102 (2002).
25. York, D. M., Lee, T.-S. & Yang, W. Quantum mechanical treatment of biological macromolecules in solution using linear-scaling electronic structure methods. *Phys. Rev. Lett.* **80**, 5011–5014 (1998).
26. Elhadj, S., Singh, G. & Saraf, R. F. Optical properties of an immobilized DNA monolayer from 255 to 700 nm. *Langmuir* **20**, 5539–5543 (2004).
27. Barnes, N. R., Schreiner, A. F., Finnegan, M. G. & Johnson, M. K. Insight into externally bound 5,10,15,20-tetrakis(2-N-methylpyridyl)porphyrinatopalladium(II), PdP(2), with B-form DNA duplexes poly(G-C)2, poly(A-T)2, and CT DNA by using combined MCD, CD, and optical data. *Biospectroscopy* **4**, 341–352 (1998).
28. Kotlyar, A. B., Borovok, N., Molotsky, T., Fadeev, L. & Gozin, M. In vitro synthesis of uniform poly(dG)–poly(dC) by Klenow exo- fragment of polymerase I. *Nucleic Acids Res.* **33**, 525–535 (2005).
29. Cuniberti, G., Craco, L., Porath, D. & Dekker, C. Backbone-induced semiconducting behavior in short DNA wires. *Phys. Rev. B* **65**, R241314 (2002).
30. Mehrez, H. & Anantram, M. P. Interbase electronic coupling for transport through DNA. *Phys. Rev. B* **71**, 115405 (2005).
31. Hübsch, A., Endres, R. G., Cox, D. L. & Singh, R. R. P. Optical conductivity of wet DNA. *Phys. Rev. Lett.* **94**, 178102 (2005).
32. Barnett, R. N. *et al.* Effect of base sequence and hydration on the electronic and hole transport properties of duplex DNA: Theory and experiment. *J. Phys. Chem. A* **107**, 3525–3537 (2003).
33. Hanna, A. E. & Tinkham, M. Variation of the Coulomb staircase in a two-junction system by fractional electron charge. *Phys. Rev. B* **44**, 5919–5922 (1991).
34. Millo, O. *et al.* Charging and quantum size effects in tunnelling and optical spectroscopy of CdSe nanorods. *Nanotechnology* **15**, R1–R6 (2004).
35. Cavazzoni, C. & Chiarotti, G. L. A parallel and modular Car-Parrinello code. *Comput. Phys. Commun.* **123**, 56–76 (1999).
36. Giannozzi, P., de Angelis, F. & Car, R. First-principle molecular dynamics with ultrasoft pseudopotentials: Parallel implementation and application to extended bioinorganic systems. *J. Chem. Phys.* **120**, 5903–5915 (2004).
37. Perdew, J. P., Burke, K. & Ernzerhof, M. Generalized gradient approximation made simple. *Phys. Rev. Lett.* **77**, 3865–3868 (1996).
38. Vanderbilt, D. Soft self-consistent pseudopotentials in a generalized eigenvalue formalism. *Phys. Rev. B* **41**, 7892–7895 (1990).
39. Lu, X.-J. & Olson, W. K. 3DNA: A software package for the analysis, rebuilding and visualization of three-dimensional nucleic acid structures. *Nucleic Acids Res.* **31**, 5108–5121 (2003).

Acknowledgements

We thank I. Brodsky, A. Migliore, M. Cavallari and O. Millo for fruitful discussions, and laboratory and computational help. Funding was provided by the EC through contracts IST-2001-38951 ('DNA-Based Nanowires') and FP6-029192 ('DNA-Based Nanodevices'). Computer time was provided by CINECA (Bologna) and by INFN-CNR through National Supercomputing Projects. Correspondence and requests for materials should be addressed to D.P. or R.D.F. Supplementary Information accompanies this paper on www.nature.com/naturematerials.

Author contributions

E.S. carried out all of the measurements, analysed the data and participated in writing the experimental paragraphs of the paper. H.C. collaborated in the set-up of the experiments and in the development of sample preparation. A.C. and C.C. carried out the calculations. A.C. participated in the analysis of the computational results. D.A.R. and G.C. participated in the theoretical interpretation. A.K. produced the poly(dG)–poly(dC) molecules. R.D.F. designed and guided the theoretical part and carried out the computational analysis and interpretation. D.P. designed and guided the whole work and in particular the experimental part and its analysis. R.D.F. and D.P. wrote the paper.

Reprints and permission information is available online at <http://npg.nature.com/reprintsandpermissions/>